Ingenieure ohne Grenzen e. V.
Grüner Weg 11, 35041 Marburg
www.ingenieure-ohne-grenzen.org

A Novel Type of Thermal Solar Water Disinfection Unit

J. Dietl, H. Engelbart, A. Sielaff
for Engineers without Borders Germany, Local Chapter Darmstadt

March 26, 2015

Abstract

A novel type of solar thermal water disinfection unit is presented in this work. The system is safe and easy to use and can be built with basic tools and widely available materials. In the unit, water is disinfected by temperature increase up to the boiling point and output is controlled by the change in density.

For employing the change in density to control the water output, a dimensioning procedure is suggested, giving the required height of the water reservoir, the heating section and the rising tube. Computational fluid dynamics simulations were performed to calculate the temperature increase in the rising tube, as it follows the temperature increase in the heated section. A model is presented to predict the water output and find a cost-effective configuration.

For heating the water a simple flat plate absorber was designed and tested. With approximately 2 square meters of absorber area, up to 50 liters water output are expected per day in regions with high solar irradiation. The system was tested with contaminated water from the sewage and a reduction to zero coliform bacteria/100 ml was obtained. In order to promote the distribution of the system, a construction manual is in the design process.

1 Introduction

Access to safe water is considered a fundamental human right and a requirement for battling poverty as well as developing sustainable societies. Worldwide, approximately 768 million people had no access to safe water in 2011 [20]. Estimated 1.5 million deaths per year are related to unsafe water, inadequate sanitation or insufficient hygiene [17]. Waterborne pathogenic microorganisms are one of the main causes of diseases related with an inadequate water supply. They include bacteria, viruses, protozoa, and helminths and are transmitted through washing, drinking or food preparation [16].

Water treatment is one step among others in a water management plan leading to a reduction in microbial contamination to a level at which the water can be considered to be safe for consumption. There exist many ways of treating water which can be categorized in the classes chemical, filtration, thermal and methods based on UV-radiation. An overview over the different methods are given among others by Okpara et al. [15] or Hörmann [10]. Generally, it can be said that there is not the one method to disinfect water but the method should be selected according to the available resources and user group.

Thermal disinfection is based on the sensitivity of microorganisms on temperature. As advantages Backer [7] names that thermal disinfection

- does not influence taste, smell or appearance
- is a single step process inactivating all pathogens
- is not affected by contaminants or particles in its ability to disinfect water.

Several studies have been performed to investigate the influence of temperature on pathogenic agents. Many microorganisms and viruses can be deactivated at temperatures well below the boiling point with enough time given. The time required to deactivate a certain pathogen decreases with increasing temperature. At the boiling point at $\approx 100\,^{\circ}\mathrm{C}$, the time required to kill most pathogens is so short that the time required for the heating process is sufficient to treat the water [7], [9]. Disinfection through boiling is employed by 50% of the world's population as one way of disinfecting water [14].

On the downside the burning of biomass-fuel for heating the water can contribute to deforestation and desertification and the inhalation of smoke resulting from burning of fuels can lead to health problems [15][18]. Employing renewable energy for heating the water can solve some of the problems related with disinfection through boiling. Areas where access to safe water is difficult often lie in regions with rather high solar irradiation. Therefore, using solar energy as power source for disinfection through heat seems to be a promising approach. Concepts following this approach were already presented, such as the solar box [6], flat plate pasteurizer [5], solar funnel cooker [11], or the solar puddle [2] without being exhaus-

tive. A review on solar thermal water disinfection concepts is given by Burch [4]. More recently, an advanced thermal water disinfection unit was developed by Konersmann and Frank [13] and is successfully installed and operated at several locations through the water kiosk foundation.

Even though several systems have been developed in the past, we still see room for improvement concerning availability, reliability and safety in case of low cost solutions that can be built completely with locally available materials. We are aiming at a system working without thermal control valves and parts that are difficult to obtain. As it is difficult to assess whether the water was hold at a specific temperature for a certain time period for flow-through systems, our goal is heating the water to the boiling point, even though thermal losses increase. Furthermore the system should be simple enough to be built by amateurs with some experience in handwork. By this, the technology can spread more easily. A construction manual will be published to promote self-construction of the unit.

In this work we present a novel system for thermal treatment of water with solar energy which was developed and tested by **Engineers without Borders Germany** in Darmstadt.

2 Concept for thermal solar water disinfection unit

The aim is the design of a unit employing solar energy to heat water to the boiling point. It should fulfill the following specifications:

- heat water to the boiling point
- capacity of 20 to 30 liters a day in average
- employment of materials widely available
- material costs below 200 €

Furthermore it should be

- simple to build
- safe and simple in usage
- cost-efficient

The following boundary conditions are adapted from the situation which can be found for families in rural areas of central Africa obtaining water from cisterns.

- no electric or pumping power available
- the water source is
  - free of chemical pollution
  - of low turbidity
  - soft (low mineral content)
- the unit is located between the 40th degree of latitude north and south

From a technical perspective the problem can be divided in two main aspects, which are heating the water to the boiling point and controlling the output of water such that only boiling hot water is released. For heating the water with solar energy, the concept of a flat plate solar collector absorber was chosen. Flat plate absorbers are widely employed in many applications and in principle do not require sophisticated manufacturing technology. They can also make use of scattered radiation for heating and do not require an exact orientation relative to the sun. In order to make sure that the water released is at saturation temperature, gravity together with the change in density due to vapor production is utilized as mean of pumping the hot water. This ensures that the water reached the boiling point and implies safety in case of failure of the unit, as no water output is produced in this case. Figure 1 demonstrates the concept of pumping the hot water.

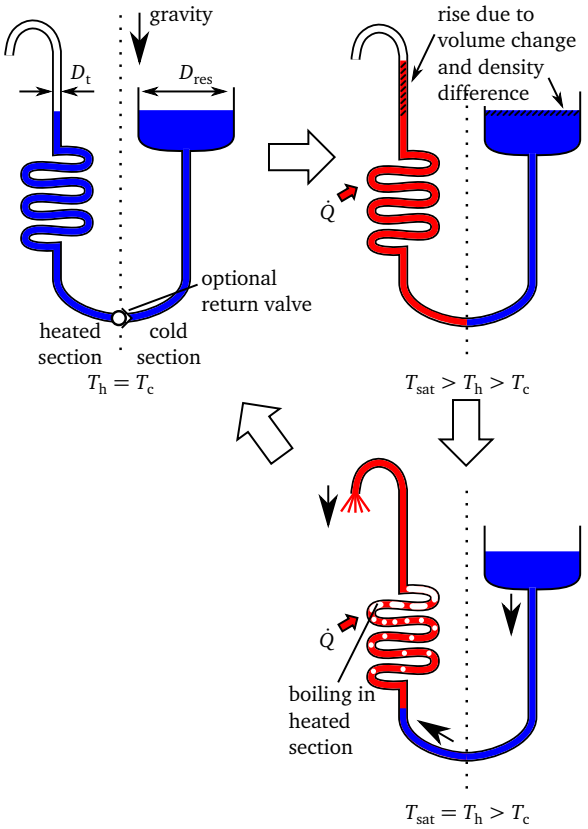

Figure 1: Concept for controlling water output

The hydrodynamic system has two branches, one with the heated section and one with the water reservoir containing the water to be heated. With the change in density due to the increase in temperature in the heated section, the water will rise in this branch. Density change due to temperature increase to saturation temperature is about 5%, degassing of dissolved air in the water can add another 3%. In the design it has to be made sure that this density change is not leading to water output. Once the water begins to boil, density will change drastically as the density ratio of vapor to liquid water is $\rho_v/\rho_w \approx 0.0006$. In order of the density change due to the production of vapor to become effective, the vapor must be hindered to rise and leave the system. With tubes in the heat-

ing section being of capillary scale, this can be guaranteed. In practice, vapor production is much faster than the rise of bubbles through the water also in bigger tubes, reducing the requirements on the size of the hydraulic structure. Together with the hot water the vapor is pushed out of the collector and new water can flow from the reservoir tank into the heated section.

Instead of using gravity as only mean of pumping the water, the system can be combined with a return valve. In this case, the water is pushed out by the increase in volume only. Introducing a return valve can increase the water output as less vapor is required and the system can operate at lower average temperatures. With a return valve, it is difficult to prevent the output of cold water at the beginning of the heating procedure (first flush). Therefore other forms of precautions have to be taken then, such that the first water output of a newly refilled unit is disinfected by other means or not consumed. Both systems were tested and the version without a return valve will be published in a construction manual for simplicity without arguing that the introduction of a return valve could not be beneficial.

A combination of the solutions for heating the water and controlling the output leads to the system depicted in Figure 2.

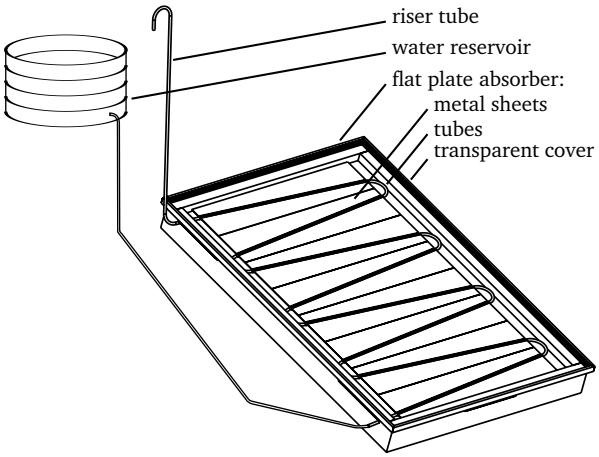

Figure 2: Principal solution

The flat plate absorber consists of metal sheets which are connected with the tube. A two layer transparent cover together with insulating material at the sides and below is required to reach saturation temperature of water. A riser tube holds the water which is pushed out of the system. The riser tube needs to be insulated carefully as well. The water reservoir needs to be on a certain level relative to the heated section and the riser tube and can be connected to the absorber through a hose. The system is free of moving parts, works without electricity and is robust and safe if implemented correctly.

In order to increase the water output, introducing a heat exchanger as employed by Konersmann and Frank [13] could be beneficial. Due to costs and complexity such a system is not included for now.

3 Modeling and Dimensioning

Hydrodynamic aspects

From a hydrodynamic perspective, some requirements on the position of the water reservoir, the outlet and the absorber have to be met, in order for the control mechanism to become effective. Figure 3 shows the most important parameters, where h is a height in direction of the gravity and l is an actual length of a certain piece of the tube. Where equations are simplified in the following, mostly the more conservative assumptions are employed. The same applies for fluid properties. The parameters are:
$h_{\mathrm{f,max}}$ - initial water level after filling,
$h_{\mathrm{f,min}}$ - minimal water level in water reservoir,
$h_{\mathrm{f,ext}}$ - water level in reservoir after thermal expansion,
h_{top} - maximal height of rising tube,
h_{out} - height of water outlet,
$h_{\mathrm{h,hi}}$ - height of top end of heated section,
$h_{\mathrm{h,low}}$ - height of lowest end of heated section,
l_{h} - tube length in heated section,
l_{htomin} - tube length from top end of heated section to position of rising tube with height $h_{\mathrm{f,min}}$,
l_{rise} - length of rising tube,
l_{htomax} - tube length from lowest end of heated section to position of rising tube with height $h_{\mathrm{f,max}}$,
l_{total} - total length of tube and hose of the system.

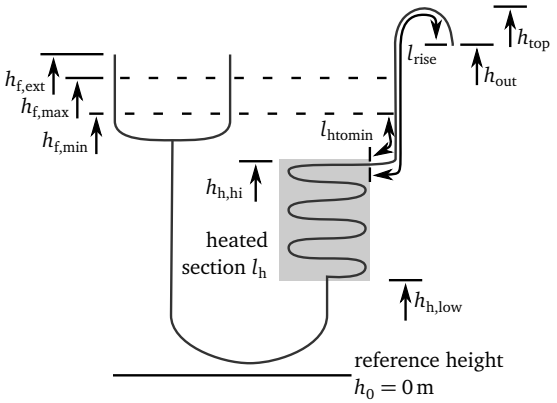

Figure 3: Heights and tube lengths

First it is undesired that due to thermal expansion and density change, water can leave the system before reaching saturation temperature. The maximal volume change without boiling to begin is given by Equation (1).

$$\Delta V = \frac{\pi}{4} D_{\mathrm{t}}^2 l_{\mathrm{htomax}} \left(\frac{\rho_{\mathrm{w,5}}}{\rho_{\mathrm{w,100}}} - 1 \right) \tag{1}$$

$\rho_{\mathrm{w,5}} \approx 1000\,\mathrm{kg/m^3}$ is the density of water at a temperature of 5 °C saturated with air, while $\rho_{\mathrm{w,100}} \approx$

930 kg/m^3 is the density of water at a temperature of 100 °C saturated with air, but with the excess air from the difference in solubility of the air at the different temperatures being present as small bubbles. The hydrostatic equilibrium results in Equation (2)

$$\left(h_{\text{out}} - h_{\text{h,low}}\right) g \rho_{\text{w,100}} - \sigma\kappa = \left(h_{\text{f,ext}} - h_{\text{h,low}}\right) g \rho_{\text{w,5}} \quad (2)$$

with the curvature of the liquid vapor interface in the tube given by $\kappa \approx \frac{4 \cdot \cos\Theta}{D_{\text{t}}}$. For a vertical riser tube and circular reservoir with diameter D_{f}, the acceptable change in volume is given by Equation (3).

$$\Delta V = \frac{\pi}{4} D_{\text{f}}^2 \left(h_{\text{f,ext}} - h_{\text{f,max}}\right) + \frac{\pi}{4} D_{\text{t}}^2 \left(h_{\text{out}} - h_{\text{f,max}}\right) \quad (3)$$

With Equations (1)–(3) h_{out} and $h_{\text{f,ext}}$ can be calculated. For the case of $D_{\text{f}} >> D_{\text{t}}$ and the tube diameter being above 0.005 m $< D_{\text{t}}$ and consequently $\sigma\kappa$ being small, the requirement for h_{out} can be calculated with the simplified Equation (4).

$$h_{\text{out}} - h_{\text{f,max}} \approx \left(h_{\text{f,max}} - h_{\text{h,low}}\right) \cdot 0.07 \quad (4)$$

In this case $h_{\text{f,ext}}$ can be taken to approximately being equal to $h_{\text{f,max}}$.

The second requirement is that for any fluid level in the reservoir, enough water should be pushed out with the vapor, such that most of thermal energy is used to heat up the water and not for phase change. The heat required for evaporation is given by Equation (5),

$$Q_{\text{evap}} = V_{\text{vapor}} \rho_{\text{v}} \Delta h_{\text{v}} \quad (5)$$

and the sensible heat to increase the temperature up to saturation temperature is given by Equation (6).

$$Q_{\text{sensible}} = V_{\text{out}} \rho_{\text{w}} c_{\text{w}} \Delta T_{\text{w}} \quad (6)$$

With the simplifications made for obtaining Equation (4), employing $\rho_{\text{v}} \ll \rho_{\text{w}}$ and assuming the vapor is only located inside the heated section, the maximal vapor volume required to push out the water can be estimated with Equation (7).

$$V_{\text{vapor}} \approx \frac{h_{\text{top}} - h_{\text{f,min}}}{h_{\text{h,hi}} - h_{\text{h,low}}} \frac{\pi}{4} D_{\text{t}}^2 l_{\text{h}} \quad (7)$$

As a larger value of h_{top} only increases the vapor required to push out the water, it should be kept as close as possible to h_{out}. The least amount of liquid being pushed out is determined by the liquid in the rising tube and given by (8),

$$V_{\text{out}} \approx \frac{\pi}{4} D_{\text{t}}^2 l_{\text{htomin}} - V_{\text{film}} \quad (8)$$

with V_{film} being the liquid volume remaining in the rising tube section. The actual two-phase flow regime during the output of the liquid and the vapor depends on solar irradiation, thermal losses and tube properties, but it should be considered that for the case of annular flow some of the liquid stays at the wall of the rising tube. Bretherton [3] gives the liquid film thickness as in Equation (9).

$$\delta_{\text{film}} = 1.34 \cdot \frac{D_{\text{t}}}{2} Ca^{2/3} \text{ with } Ca = \frac{\mu_{\text{w}} U_{\text{max}}}{\sigma} \quad (9)$$

To estimate the maximal possible flow velocity U_{max} resulting in the maximal film thickness, the rate of vapor generation is calculated from the maximal solar irradiation (substracting thermal losses) $\dot{Q}_{\text{in}}$ under the assumption that the vapor expands only in the direction of the outlet. This is leading to Equation (10) for the velocity and Equation (11) for the remaining liquid volume.

$$U_{\text{max}} \approx \frac{4 \cdot \dot{Q}_{\text{in}}}{\pi D_{\text{t}}^2 \Delta h_{\text{v}} \rho_{\text{v}}} \quad (10)$$

$$V_{\text{film}} = l_{\text{rise}} \frac{\pi}{4} \left(D_{\text{t}}^2 - \left(D_{\text{t}} - 2\delta_{\text{film}}\right)^2\right) \quad (11)$$

It also should be considered that if $h_{\text{top}} - h_{\text{f,min}} = h_{\text{h,hi}} - h_{\text{h,low}}$ the heated section completely fills with vapor without water being pushed out.

Finally, the maximal possible output of the system is not only limited by heat input but also by the flow resistance of the tubes. Once the water is faster heated up and evaporated than flowing through the absorber, no more water can be pushed out. The point where this happens is approximately given by Equation (12),

$$\frac{\pi}{128} D_{\text{t}}^4 \frac{\Delta p}{\mu_{\text{w}} l_{\text{total}}} = \frac{\dot{Q}_{\text{in}}}{\rho_{\text{w}} \Delta h_{\text{v}} + \rho_{\text{w}} c_{\text{w}} \Delta T_{\text{w}}} \quad (12)$$

calculated with the friction factor for laminar flow $f = 64/Re$. The maximal driving pressure difference is given by $\Delta p = \rho_{\text{w}} g (h_{\text{f,min}} - h_{\text{h,hi}})$. In practice, the left side of Equation (12) will be much larger than the right side of the equation, unless there are very sharp bends in the tube or hose, leading to an additional pressure drop or the system is scaled up to very large sizes.

Temperature in the rising tube

During operation, the rising tube will hold some water which was heated up in the heated section beforehand. As there will be thermal losses to the surroundings the water will eventually cool down again and once vapor is generated in the heated section the water might be pushed out at lower temperatures than saturation temperature. As the water was heated up to saturation temperature before, it is still disinfected, but if the system was completely dry and filled for the

first time with water, it might be pushed out without ever been heated to saturation temperature.

The water in the rising tube is only heated by conduction through the tube and free convection of water from the heated section. In order to determine whether free convection is sufficient to heat the water in the rising tube, a numerical simulation of the flow in the rising tube was performed. The simulation was performed with the free finite volume CFD software OpenFOAM. The solver employed is based on the solver "chtMultiRegionFoam". Figure 4 shows the computational domain.

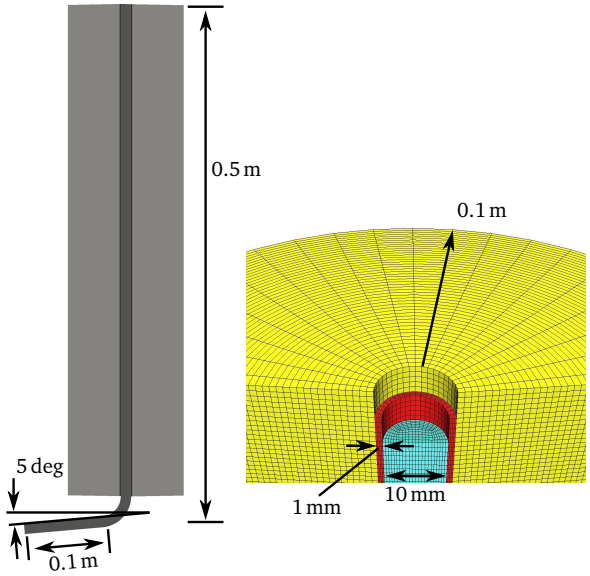

Figure 4: Computational domain and mesh

The fluid domain consists of a vertical part and a almost horizontal part with a slope of 5 deg. The vertical part is surrounded by a copper tube which again is surrounded by insulation. On the outside of the insulation a convective boundary condition is applied with a free stream temperature of 20 °C and a heat transfer coefficient of 32 W/m^{2}K, which is approximately the value for a wind speed of 5.5 m/s. At the bottom end of the fluid region, a fixed pressure boundary condition is set with fluid being allowed to flow in and out. The temperature of the fluid intake is varied with time to simulate the temperature rise at the absorber. The rate of temperature increase is taken from the fastest heating experimentally observed and set to 0.01 °C/s.

Initially fluid and solid regions are set to a temperature of 20 °C and the temperature at the inlet is set to 25 °C. Liquid properties are those of water with a temperature dependent Prandtl Number being implemented.

A mesh convergence study was performed and the selected mesh is depicted in Figure 4. The temperature and flow field after a time of 50 minutes is shown in Figure 5.

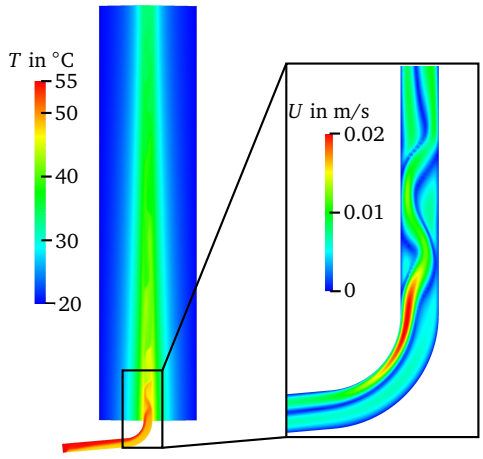

Figure 5: Temperature and flow field after 50 minutes

Hot liquid is rising while cold liquid is dropping, leading to the temperature gradient in the tube. As can be taken from the simulations, the convective boundary condition has no influence on the heating process in this initial phase, as the insulation only slowly heats up and the outside stays at the initial temperature.

Figure 6 shows the development of the temperature at the inlet, at the top end of the tube and the average temperature in the almost horizontal section for the entire time.

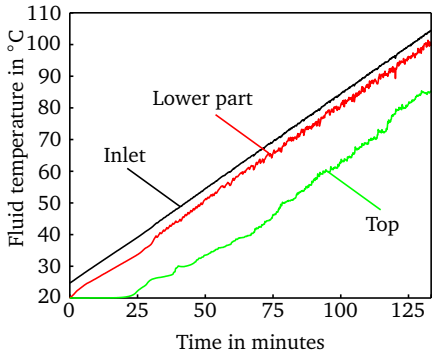

Figure 6: Temperature evolution over time

The temperature fluctuations are caused by convective plumes rising in the tube. The temperature difference between inlet and top decreases slightly with time due to the increasing Prandtl number of water with temperature. Once the water temperature reaches 100 °C at the inlet, the temperature difference between the top and the bottom is approximately 18 °C. The results show that for the given configuration, the temperature of the water in the rising tube should be sufficiently high. They also show that for a higher filling level, thinner tubes or a longer horizontal adiabatic section between the heated part of the unit and the rising tube, the temperature will most likely be not sufficiently high in all parts of the tube.

Furthermore, the rate of temperature increase at the inlet might be even higher if the distance between the tubes in the heating section is increased. In order to allow the water in the rising tube to be heated before the first output is produced, it has to be made sure that the water temperature is highest at the upper end of the absorber. As will be shown in the measurement section, this is not necessarily the case, as the slope of the tube is rather low and additional energy is required to heat the water in the rising tube. Therefore during the design of the absorber, measures have to be taken to provide a larger heat flow to the upper part of the tube in the absorber.

For the case that the water can not be sufficiently heated by free convection, the very first output of water after refilling a dry unit needs to be disposed.

Thermal modeling and optimization

For thermal optimization of the system, a simple numerical model was created. In the development process, modeling went hand in hand with the detailed designing of the unit with the results presented in section 4. For modeling as well as designing of the unit, the scriptum to the lecture "Solartechnik I" of Dr.-Ing. Harald Drück from Stuttgart University was of great help. Calculation of solar irradiation based on collector position and orientation was taken from Gassel [8].

From experiments it is known that the temperature gradient from the inlet to the outlet is much larger than the temperature gradient across the metal sheet. Therefore the system is discretized in direction of the flow as shown in Figure 7.

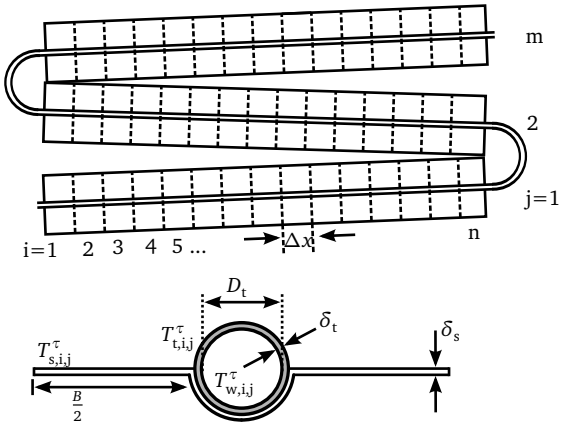

Figure 7: Discretisation for modeling

Each of m metal sheets is discretized into n elements which include the water and the tube in this section. $T^\tau_{w,i,j}$, $T^\tau_{t,i,j}$, $T^\tau_{s,i,j}$ are the water, tube and metal sheet temperature of element i,j at time τ.

In the following, the modeling equations will be given for a central element. For boundary elements appropriate boundary conditions have to be considered. The energy equation for the water element in its implicit form is given by Equation (13).

$$\rho_w c_w \Delta x \frac{\pi}{4} D_t^2 \frac{T^\tau_{w,i,j} - T^{\tau-\Delta\tau}_{w,i,j}}{\Delta\tau} = \frac{\lambda_w \pi D_t^2}{4\Delta x}\left(T^\tau_{w,i-1,j} + T^\tau_{w,i+1,j} - 2T^\tau_{w,i,j}\right) + \alpha_w \pi \Delta x D_t \left(T^\tau_{t,i,j} - T^\tau_{w,i,j}\right) \quad (13)$$

The heat transfer coefficient α_w depends on geometry and liquid properties as well as flow conditions and temperatures. As those are not well enough known, the value is simply set to a value of $\alpha_w = 500\,\mathrm{W/m^2K}$ leading to a smaller thermal resistance than the resistance between tube and metal sheet. Such a value can be considered to be rather low for two phase flow but significantly larger than single phase free convection.

Free convection in flow direction is neglected in this case due to the low slope of the tubes. Instead, the water is assumed to flow only once enough vapor is created. In this case the temperature profile of the water is explicitly moved downstream according to the amount of water output. Insulation through vapor in the tube as well es movement of water for very slow vapor bubble growth is not considered.

Equation (14) gives the energy equation for one tube element.

$$\rho_t c_t \Delta x \frac{\pi}{4}\left(\left(D_t + 2\delta_t\right)^2 - D_t^2\right)\frac{T^\tau_{t,i,j} - T^{\tau-\Delta\tau}_{t,i,j}}{\Delta\tau} = \frac{\lambda_t \pi\left(\left(D_t + 2\delta_t\right)^2 - D_t^2\right)}{4\Delta x}\left(T^\tau_{t,i-1,j} + T^\tau_{t,i+1,j} - 2T^\tau_{t,i,j}\right) - \alpha_w \pi \Delta x D_t \left(T^\tau_{t,i,j} - T^\tau_{w,i,j}\right) - \frac{\pi \Delta x \left(D_t + 2\delta_t\right)}{2R_{ts}}\left(T^\tau_{t,i,j} - T^\tau_{s,i,j}\right) + q_{in}\Delta x\left(D_t + 2\delta_t\right) - \alpha_{s,eff}\Delta x\left(D_t + 2\delta_t\right)\left(T^\tau_{t,i,j} - T^\tau_{amb}\right) \quad (14)$$

Between tube and metal sheet, the thermal resistance R_{ts} is introduced, which depends on the bonding technique and thermal properties of the metals. As the tube is only one numerical cell thick, the thermal conductivity of the tube has to be considered in the thermal resistance R_{ts} and in the heat transfer coefficient α_w between tube and water. Half of the tube is exposed to the solar irradiation q_{in}. The effective heat transfer coefficient $\alpha_{s,eff}$ to the surroundings, which is equivalent to a thermal loss coefficient, is calculated according to the formula of Klein [12] (taken from [1]) and is a function of the metal temperature itself.

Finally, the energy equation for the piece of metal

sheet is given by Equation (15).

$$(\rho c)_{s,\mathrm{eff}}\Delta x\left(B+\pi\frac{D_t+2\delta_t}{2}\right)\frac{T^{\tau}_{s,i,j}-T^{\tau-\Delta\tau}_{s,i,j}}{\Delta\tau}=$$
$$\frac{\lambda_s\delta_s}{\Delta x}\left(B+\pi\frac{D_t+2\delta_t}{2}\right)\left(T^{\tau}_{s,i-1,j}+T^{\tau}_{s,i+1,j}-2T^{\tau}_{s,i,j}\right)-$$
$$\frac{\pi\Delta x\left(D_t+2\delta_t\right)}{2R_{ts}}\left(T^{\tau}_{s,i,j}-T^{\tau}_{t,i,j}\right)+$$
$$q_{in}\Delta xB-\alpha_{s,\mathrm{eff}}\Delta xB\left(T^{\tau}_{s,i,j}-T^{\tau}_{amb}\right) \quad (15)$$

The effective thermal capacity $(\rho c)_{s,\mathrm{eff}}$ includes partly the thermal capacity of the insulation material and glass cover. The system of equations can be written as a matrix equation with a vector for the temperatures to solve for. As the water output is occurring rapidly and calculated explicitly, a small time step $\Delta\tau$ has to be chosen. With the timestep being small, the temperatures of the old time $\tau-\Delta\tau$ were used to calculate the effective heat transfer coefficient $\alpha_{s,\mathrm{eff}}$ and a linear system of equations is obtained, which can be solved with a linear solver.

Validation of the model was performed with the measurement data of the first prototype built. For this, the measured solar irradiation was directly fed into the model. Figure 8 compares the measured temperature on the central metal sheet with the simulated value and Figure 9 compares the calculated water output with the measured values. The data was recorded on September 3rd 2013, N 49° 51' 37.44", E 8° 40' 42.96", starting at 8 am local summer time.

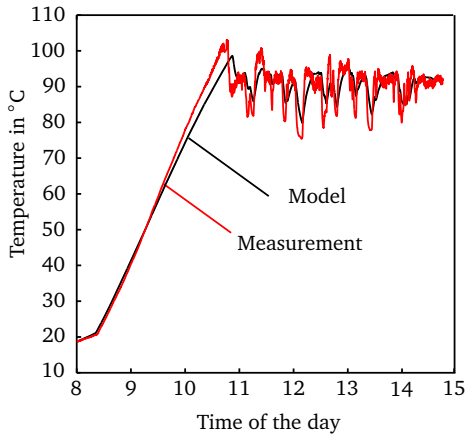

Figure 8: Temperature of central metal sheet

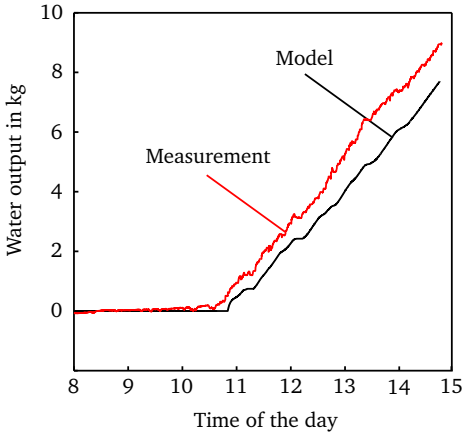

Figure 9: Water output over time

The evolution of the temperature of the central metal sheet compares very well. The measured temperature fluctuations are somewhat larger than those obtained from the model. This difference is probably due to the thermal capacity of the insulation and the glass, which is added to some extend to the metal sheet in the model.

The measured water output is somewhat larger than the output calculated from the model. There are several possible explanations for the observed difference, including measurement errors in the automated measurement system and the increased thermal capacity of the metal sheets in the model. Considering the uncertainties in the local weather conditions and material properties, which are required for a predictive calculation of the output, the agreement is sufficient to find an optimal configuration and approximate average output.

The predictive ability was tested by supplying only location, date and cloud cover to the model. For sunny days, there is almost no difference between predicted output and the output calculated with the actual measured solar irradiation. For cloudy days, employing an average value for the cloud cover leads to large differences between the output of the model and the measured output on a daily basis. The problem is that it is a huge difference for the unit whether there is a slight cloud cover all day or there are heavy clouds in the morning and no clouds in the afternoon. An average measure like the cloud cover can not account for these differences. Therefore the optimization was performed with settings for a clear sky, while the calculation for the average yearly output needs to be corrected with an experimentally determined empirical value. Figure 10 shows the measured output divided by the maximal output for a clear sky (taken from the model) over the cloud cover. The cloud cover is given in "eigths", with 0 being a clear sky and 8 being a sky completely covered. The data for the cloud cover is taken from station 1420 (Frankfurt, Germany) from

Deutscher Wetterdienst *www.dwd.de*.

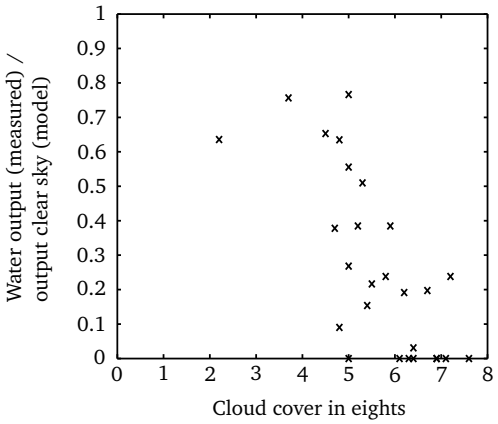

Figure 10: Reduction of water output with cloud cover

The measurement shows that above a cloud cover of 6/8, there is mostly no output. Between 5 and 6 there are large variations in the output while below 5 the unit becomes more reliable in producing water.

In order to find an optimal configuration for the given conditions and desired output, the thermal model was combined with cost functions for the materials required. Of course, the cost functions do have a high incertitude but still they offer a basis for the decisions. As an example, Figure 11 shows the approximate specific investment costs for each liter of water produced per day for an absorber of fixed sized but with different numbers of metal sheets.

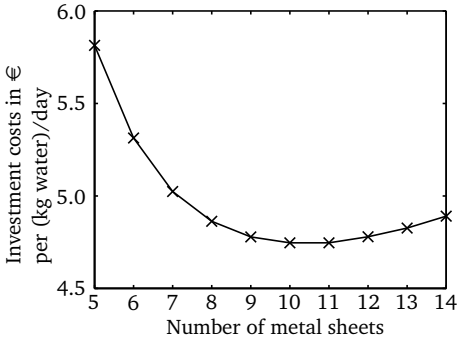

Figure 11: Optimization example

Increasing the number of metal sheets increases the thermal efficiency but also increases the tube length. With copper tube being a large expanse factor, this increases the investment costs. The minimal specific costs can be found at 10 sheets with costs increasing only mildly afterwards. As more sheets require more effort in fabricating the absorber, 8 sheets were selected with costs being close to the minimum.

Suggestion for dimensioning procedure

From the equations and models presented in this section, a basic dimensioning procedure can be deduced. First, the size of the absorber should be selected according to the water output required and the location. If possible, a cost optimization should be performed which results in a certain tube length. If such an optimization goes beyond the scope of the project, Figure 12 can be used to find the maximal water output for the absorber presented in the next section.

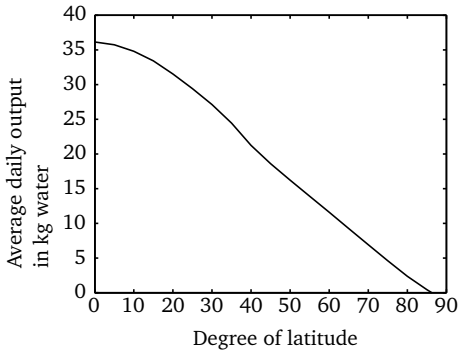

Figure 12: Average output per day

The graph was created with the model presented before, presuming optimal conditions, meaning no wind and a clear sky. The daily water output was averaged over one year. The actual average output will be significantly lower depending on the local climate. It is very likely that the average output will be less than half of the value in Figure 12. If local weather data is available, a rough estimation is possible with the information given in Figure 10.

The optimal tilting angle depends on the location, a guide value can be taken from Equation 16.

$$\text{tilting angle (deg)} = \frac{1}{3} \cdot \text{latitude (deg)} + 20\,\text{deg} \quad (16)$$

On the northern hemisphere, the absorber should face south, on the southern hemisphere north. It has to be considered that the vertical height of the absorber has to be at least the distance between the top of the rising tube and the lower end of the reservoir, if possible much larger. For this reason, a rectangular shape with the long side pointing in rising direction is preferable. The water reservoir should be as shallow as possible.

In order to allow the water in the rising tube to be heated by free convection from the absorber, the rising tube should be kept as short as possible. From Equations (4) to (11), the position of the water reservoir and the length of the rising tube can be calculated. The following iterative steps can be taken:

1. select an absorber size with area A_h and calculate the length of the tube in the absorber l_h

2. select a shallow water reservoir of appropriate volume (holding enough water for at least one day of operation) to obtain $h_{\mathrm{f,max}} - h_{\mathrm{f,min}}$

3. calculate the vapor velocity $U_{\max}$ with Equation (10), approximating $\dot{Q}_{\mathrm{in}} \approx 300\,\mathrm{W/m^2} \cdot A_{\mathrm{h}}$.

4. calculate the maximal film thickness δ_{film} with Equation (9)

The iteration can be started with a tilting angle of the absorber taken from Equation 16, but between the lowest and the highest point of the absorber $h_{\mathrm{h,hi}} - h_{\mathrm{h,low}}$ a distance of at least twice the height of the water reservoir $h_{\mathrm{f,max}} - h_{\mathrm{f,min}}$ should be selected at the beginning. The length of the rising tube l_{rise} can be set to be twice the reservoir height $h_{\mathrm{f,max}} - h_{\mathrm{f,min}}$ plus the approximate level increase due to water expansion $0.07 \cdot (h_{\mathrm{h,hi}} - h_{\mathrm{h,low}})$.

5. calculate the volume of the liquid film V_{film} with Equation (11).

6. solve for $h_{\mathrm{f,min}}$. For this Equations (5) to (8) need to be combined employing $Q_{\mathrm{evap}}/Q_{\mathrm{sensible}} = 0.1$, $\Delta T_{\mathrm{w}} = 80$, $l_{\mathrm{htomin}} \approx h_{\mathrm{f,min}} - h_{\mathrm{h,hi}}$, leading to

$$h_{\mathrm{f,min}} = \left(0.042 \cdot l_{\mathrm{h}} \frac{l_{rise} + h_{\mathrm{h,hi}}}{h_{\mathrm{h,hi}} - h_{\mathrm{h,low}}} + h_{\mathrm{h,hi}} + \frac{4V_{\mathrm{film}}}{\pi D_{\mathrm{t}}^2}\right) / \left(1 + 0.042 \cdot l_{\mathrm{h}} \frac{1}{h_{\mathrm{h,hi}} - h_{\mathrm{h,low}}}\right) \quad (17)$$

7. with this, the height of the reservoir $h_{\mathrm{f,max}}$ is given, too and the required height of the rising tube h_{out} can be calculated by solving Equation (4).

8. update the length of the rising tube $l_{\mathrm{rise}} \approx h_{\mathrm{out}} - h_{\mathrm{h,hi}}$

If $h_{\mathrm{out}} - h_{\mathrm{h,hi}} > 0.5\,\mathrm{m}$ with a tube diameter of 0.01 m, $h_{\mathrm{out}} - h_{\mathrm{f,min}}$ is too large and a more shallow reservoir needs to be installed. Alternatively increasing the tilting angle or the length of the absorber in rising direction can also help. The same applies if $\frac{l_{\mathrm{rise}} + h_{\mathrm{h,hi}} - h_{\mathrm{f,min}}}{h_{\mathrm{h,hi}} - h_{\mathrm{h,low}}} > 2/3$. If $h_{\mathrm{out}} - h_{\mathrm{h,hi}}$ is much shorter than 0.5 , $h_{\mathrm{f,min}}$ can be increased to improve the efficiency of the unit.

Check that the left side of Equation (12) is a magnitude higher than the right side. Otherwise $h_{\mathrm{f,min}} - h_{\mathrm{h,hi}}$ needs to be increased or the tube length decreased.

Repeat steps 5 to 8 at least once or until appropriate values are found.

With some absorber designs and boundary conditions, the method explained above might not lead to a satisfying result. In this case the factor $Q_{\mathrm{evap}}/Q_{\mathrm{sensible}}$ might need to be increases or accepted that the very first water output still might not be disinfected. In case first flush is not a problem (e.g. water is used for cooking afterwards) or the first flush can be disposed by the operator, it is suggested to include a return valve at the lowest point of the absorber. This will reduce thermal losses and mildly increase the output.

It should be noted that in any case, with or without return valve, Equation (4) needs to hold. Violating the other conditions will lead to a low output or contaminated water for a refill of a completely dry unit. In case Equation (4) is not fulfilled a constant flow of water not being at saturation temperature can be the consequence.

4 Construction

In the following, the design of the unit will be described. Depending on the availability and costs of materials, parts or tools, other implementations of the principal solution might be beneficial. If available, also vacuum tubes or readily built high temperature solar absorbers can be used. Our goal was the design of a simple unit which can be built at low costs at the expense of efficiency to some extend.

Figure 13 shows a sectional view of the absorber unit.

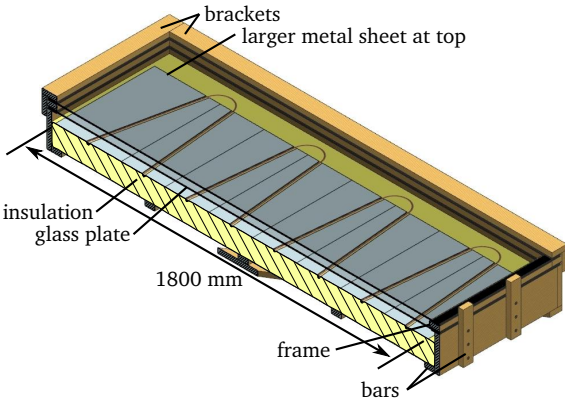

Figure 13: CAD drawing of collector design

The absorber is 1.8 m times 1 m, consisting of 8 aluminum sheets holding the copper tube. The metal sheet at the top is larger to allow heating of the water in the rising tube. Aluminum was selected due to its high thermal conductivity, low thermal capacity and rather low costs. In order to be able to shape the sheets with simple tools, thickness should be equal or below 0.8 mm. Into each sheet, a groove is pressed, holding the tube.

The tube is bended into a meander shape, rising only slightly on each metal sheet. As depicted in Figure 14, the tube is fixed with a wire to the metal.

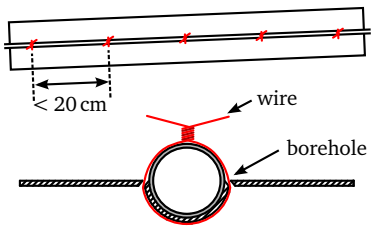

Figure 14: Wire bonding technique

For this, two little holes are drilled into the metal right next to the tube at least every 20 cm on the metal sheet. The wire is put through the holes around the tube and drilled to press the tube onto the metal. A complete contact between tube and metal is desired. Usually, tubes are welded to the metal on flat plate absorbers, but this requires sophisticated tools and skills and puts more constraints on the pairing of the materials. The meander shape was selected due to the simpler fabrication compared to a harp. The horizontal arrangement of the metal sheets allows a larger temperature gradient between the top and the bottom, decreasing thermal losses. If no copper tubes are available, bending might be difficult and a harp has to be built. It is required that the tubular system is pressure-tight, as it needs to hold the vapor. In order to make sure that enough power is provided to the rising tube and that the highest temperature in the fluid is at the top, the area of the top metal sheet was increased by 50%.

Below the absorber, 10 cm of insulation is placed, for which hemp or mineral wool can be employed. The absorber with the insulation is placed in a wooden box. At the bottom of the box, a metal grid or wooden bars carry the insulation and the absorber. On top of the box, a glass plate is put, separated by some insulation material from the wood. A wooden frame is put on the glass and another glass plate is put on this frame. Again, the glass is always separated by some insulation material from the wood. For the glass plates, common 4 mm window glass was employed. The insulation material between wood and glass reduces thermal losses and the risk of cracking of the glass.

On the upper end and on the side ends, wooden brackets are pressed on the glass and are fixed with screws pointing sideways into the wooden box. At the lower end, the glass is only hold by some vertical bars to prevent it from sliding down from the box. This is necessary to allow water to run from the glass.

The rising tube is located outside of the box on the side. Care should be taken that the rising tube is well insulated and that there is always a positive slope of the tube section between the absorber and the vertical rising tube. In our case, 5 cm of hemp wool was wrapped around the tube and plastic foil was wrapped around the insulation to keep it dry. The metal absorber and tube were colored with black stove enamel. The foil at the rising tube was colored as well, to protect it from UV-radiation. At the feed through of the tube, the tube needs to be insulated against the wood and rain water has to be hindered to enter the box.

If hard water is used with the unit, scaling can occur, increasing thermal resistance and decreasing the output. In that case, the tube has to be exchanged after some time. Safety of the concept should not be impaired by scaling. In regions with termites being a problem, wood needs to be treated.

5 Measurements and microbiological proof of concept

Two prototypes were built for performing thermal and microbiological measurements. First tests and thermal measurements were performed with a scaled down version of the system. Figure 15 shows the first prototype which was built during the development process together with the measurement positions.

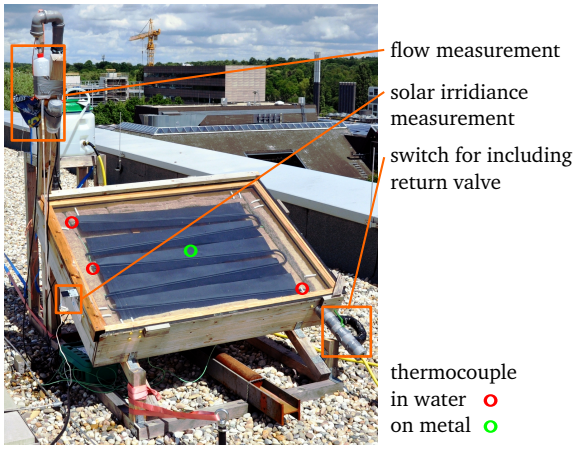

Figure 15: First prototype after first year of measurements

A valve was included to switch between an open system and a system with return valve. The solar irradiation was measured with a simple photo-voltaic cell, which was calibrated against a pyranometer. The output was collected in a small bottle with a pressure sensor giving the filling height of the bottle. Once the bottle was full a valve opened, allowing the water to flow from the bottle back into the water reservoir. Type K thermocouples were calibrated and mounted into the flow and on the metal to record temperatures. A *NI Wireless Sensor Network* system was used to collect and transmit the data. Figure 16 shows temperatures at the different measurement positions for September 4th, 2013, between 10 am and 5 pm.

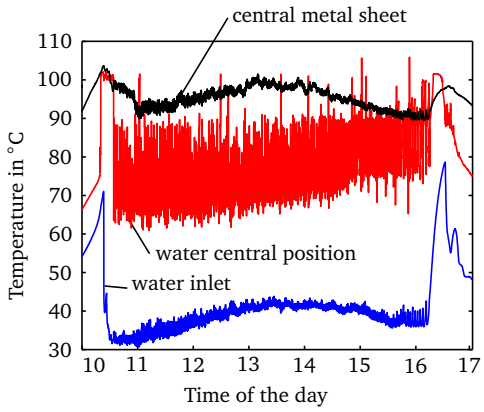

Figure 16: Temperature measurements

In the morning, the system is heating up with a slight temperature gradient between the top and the bottom. Once water is put out for the first time, a temperature jump can be observed at the central position. This behavior is due to the movement of hot water or steam from the section connected to the metal to the tube coupling containing the thermocouple. The jump of the temperature to saturation temperature shows that saturation temperature was reached first in the central section. At the lowest measurement position a sudden temperature decrease can be observed as cold water is entering the unit. During operation of the system, temperature fluctuations can be observed at the central measurement position as water is pushed out of the system in a batch process. Between the metal sheet and the water in the central section, an average temperature gradient of about 20 °C can be observed.

In order to assess the difference between a system with return valve and an open system, the output was measured by hand with a measuring jug with alternating switch for including the valve. Figure 17 shows the measured water batches over time with and without return valve.

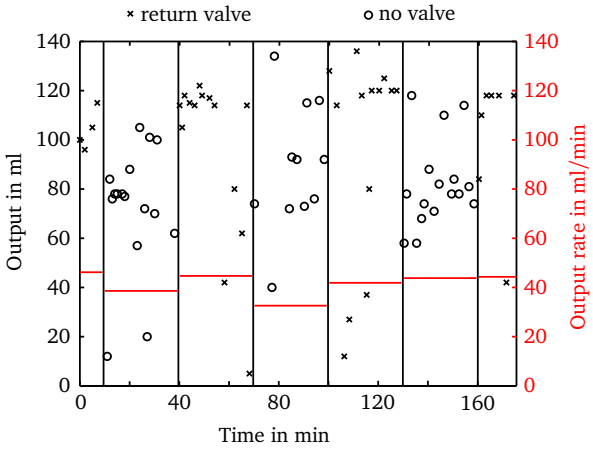

Figure 17: Output with and without return valve

With return valve, the individual water batches and also the output rate is larger than without return valve. Without return valve, the created vapor also extends downwards to cooler sections of the absorber, leading to condensation and higher average absorber temperatures. The average output rate with return valve was measured to be $0.74 \cdot 10^{-3}$ kg/s and without valve $0.64 \cdot 10^{-3}$ kg/s.

During the time of testing, some condensation of water occurred at some days in the morning between the glass sheets. The condensate was located at the lower end of the unit, but disappeared quickly when temperature increased, even without additional ventilation holes.

In order to prove the concept, introduce changes in the design and to assess the problematic of the first flush, a second prototype was built at full scale and fed with contaminated water from the sewage. Over a period of one month, the microbial contamination of the water was measured. The absorber was emptied each night and refilled with contaminated water afterwards. In the morning the contamination of the water in the water reservoir as well as the contamination of the first water output from the unit was measured. After that, the water output was collected over the day and the contamination of this mixed output was measured in the evening. Details on the measurement procedure and results can be found in the Bachelor Thesis of Fabian Thiemann, written at TU Darmstadt in 2014 at the Institute IWAR. Table 1 gives an excerpt of the measurement data showing the contamination with coliform bacteria of the water input, the first water output and the total collected output. Only the data of days where a measurement of the first water output was performed are shown.

input	first output	mixed output
$4.6 \cdot 10^4$	0	0
$1.7 \cdot 10^4$	0	0
$1.4 \cdot 10^5$	0	0
$1.1 \cdot 10^5$	0	0
$2.9 \cdot 10^5$	2.0	0
$7.7 \cdot 10^6$	3.6	0
$1.1 \cdot 10^7$	7.1	0
$8.6 \cdot 10^6$	1.6	0
$7.3 \cdot 10^6$	0	0
$4.9 \cdot 10^6$	0	0

Table 1: Contamination in number of coliform bacteria/100 ml

The results show that the contamination of the mixed output is zero for all measurements taken. Only for a very high input contamination with already a high turbidity the contamination of the first output is not zero. But even for those cases the reduction in contamination is very high. Considering the fact that the first output is about 100 ml and the total output over a day is several liters, mixing the first output with the collected output would probably lead to

a measured reduction to zero of the mixed output as well.

6 Potential hazards and problems

Problems and hazards can arise during the building phase and during operation. When building a unit, general precautions have to be taken connected with operating machinery and handling tools. The tubes employed have to be free from potentially harmful contaminations. During the operation, hot water and steam leave the unit at high velocity. Precautions should be taken that the reservoir used to collect the hot water can not be tilted or hot parts of the rising tube are unconcealed. In case easily flammable materials are used and sunlight is concentrated through surface defects in the glass, the materials might ignite. If disassembled, it has to be considered that the metal sheets and glass cover can be at a high temperature. In case the height of the rising tube is too low or the water reservoir is set too high, untreated water can leave the unit after the first fill of the reservoir or even during operation. The same problem can appear if the rising tube is too high and free convection might not be sufficient to heat the water in the rising tube. If in doubt, the first water output after a refill of a completely dry unit should be disposed.

If installed correctly, the unit is able to reduce the microbial contamination. This is not implying that the water is potable after the treatment. Any chemical pollution and particles in the water can not be removed and can lead to severe health problems. As the water is not sanitized completely, microbial contamination might again increase after the treatment. If the employed water is acid, increased amounts of copper can dissolve in the water during flow through the unit. In any case, small children should not consume the water if other reliable sources are available. Any user group should be informed about safety issues and correct use of the unit.

7 Summary

Heat is widely employed for the disinfection of water, and several systems were presented in the past to employ renewable energy for the heating process. In this work, a novel thermal water disinfection unit is presented, which is safe and easy to use and can be built from materials widely available. For disinfection, the water is heated to the boiling point. A system was developed being able to control the water output based on the density difference between vapor and liquid. Dimensioning and optimization were performed with a computational model which was validated with thermal measurement data from a scaled down prototype. A full scale prototype was tested with contaminated water to prove the feasibility of the concept. Depending on the location, up to 50 liters of boiling hot water are discharged from the unit on sunny days. In order to promote self-construction, a construction manual will be published. In this paper, modeling equations together with a dimensioning procedure are given, allowing adaption of the concept to employ other materials or resizing the system.

Acknowlegments

Participants and supporters of the development process are among others:

Anna Bach
Maximilian von der Grün
Dieter Holzhäuser
Elisa Jährling
Tobias Kehl
Felix Lanfermann
Thomas von Langenthal
Tim Müller
Verena Pfeifer
Angelika Sell
Bernd Simon
Swantje Staaden
Matthias Stepper
Bastian Stumpf
Fabian Thiemann
Margo Tilghman
Julius Unrath

Financial support, materials and infrastructure were provided by

ES Electronic Sensor GmbH
HEAG Südhessische Energie AG
IDEXX Europe B.V.
Merck KGaA
National Instruments Germany GmbH
TU Darmstadt:
Department of building management
Institute IWAR
Institute PTW
Institute TTD

Nomenclature

A	area	(m^2)
c	specific heat capacity	(J/kgK)
D	diameter	(m)
h	height	(m)
l	length	(m)
p	pressure	(Pa)
Q	heat	(J)
$\dot{Q}$	heat flow	(W)
q	heat flux	(W/m^2)
R	thermal resistance	(K/W)
T	temperature	(°C)
U	velocity	(m/s)
V	volume	(m^3)
α	heat transfer coefficient	(W/m^2K)
δ	thickness	(m)
Θ	contact angle	(deg)
κ	curvature	(1/m)
λ	thermal conductivity	(W/mK)

μ	viscosity	(Pa s)
ρ	density	(kg/m^3)
σ	surface tension	(N/m)

subscripts

amb	ambient
c	cool (section)
eff	effective
f	filling level
h	heated (section)
res	reservoir
s	(metal) sheet
sat	at saturation condition
t	tube
v	vapor
w	(liquid) water

Properties of water

T_{sat}	100 °C
ρ_w	958.35 kg/m^3
ρ_v	0.59814 kg/m^3
c_w	4.217 kJ/kgK
λ_w	0.6772 W/mK
μ_w	$281.6 \cdot 10^{-6}$ Pas
σ	0.05891 N/m
Δh_v	2256.5 kJ/kg

Table 2: Properties taken from VDI heat atlas [19]

References

[1] N. Akhtar and S.C. Mullick. Computation of glass-cover temperatures and top heat loss coefficient of flat-plate solar collectors with double glazing. *Energy*, 32(7):1067–1074, 2007.

[2] D. Andreatta, D. Yegian, L. Connelly, and R. Metcalf. Recent advances in devices for the heat pasteurization of drinking water in the developing world. In *Intersociety Energy Conversion Engineering Conference*. American Institute of Aeronautics and Astronautics, 1994.

[3] F.P. Bretherton. The motion of long bubbles in tubes. *Journal of Fluid Mechanics*, 10(02):166–188, 1961.

[4] J. Burch and K.E. Thomas. An overview of water disinfection in developing countries and the potential for solar thermal water pasteurization. Technical report, National Renewable Energy Lab., Golden, CO (United States), 1998.

[5] L.F. Caslake, D.J. Connolly, V. Menon, C. Duncanson, R. Rojas, and J. Tavakoli. Disinfection of contaminated water by using solar irradiation. *Applied and Environmental Microbiology*, 70(2):1145–1151, 2004.

[6] D.A. Ciochetti and R.H. Metcalf. Pasteurization of naturally contaminated water with solar energy. *Applied and Environmental Microbiology*, 47(2):223–228, 1984.

[7] C.D. Ericsson, R. Steffen, and H. Backer. Water disinfection for international and wilderness travelers. *Clinical Infectious Diseases*, 34(3):355–364, January 2002.

[8] A. Gassel. *Beiträge zur Berechnung solarthermischer und exergieeffizienter Energiesysteme*. Dissertation, TU Dresden, 1997.

[9] C.D. Groh, D.W. MacPherson, and D.J. Groves. Effect of heat on the sterilization of artificially contaminated water. *Journal of Travel Medicine*, 3(1):11–13, 1996.

[10] A. Hoerman. *Assessment of the microbial safety of drinking water produced from surface water under field conditions*. PhD thesis, Faculty of Veterinary Medicine, University of Helsinki, 2005.

[11] S.E. Jones, J.F. Chesley, D. Hullinger, J. Winterton, J. Lawler, D. Seth, and D. Jones. The solar funnel cooker. *The Solar Archive. Solar Cookers International*, 10, 2005.

[12] S.A. Klein. Calculation of flat-plate collector loss coefficients. *Solar Energy*, 17:79, 1975.

[13] L. Konersmann and E. Frank. Solar water disinfection: field test results and implementation concepts. *Institut für Solartechnik SPF, University of Applied Science Rapperswil*, 2011.

[14] J.M. Nyagwencha, J.W. Kaluli, P.G. Home, and M. Hunja. Water and water-borne diseases in north masaba district, kenya. *Journal of Agriculture, Science and Technology*, 14(1), 2013.

[15] C.G. Okpara, N.F. Oparaku, and C.N. Ibeto. An overview of water disinfection in developing countries and potentials of renewable energy. *Journal of Environmental Science & Technology*, 4(1), 2011.

[16] World Health Organization. *Guidelines for Drinking-water Quality*. Volume 1. World Health Organization, Geneva, Switzerland, third edition, 2004.

[17] A. Pruess-Uestuen, R. Bos, F. Gore, and J. Bartram. WHO | safer water, better health, 2008.

[18] M. Tucker. Can solar cooking save the forests? *Ecological Economics*, 31:77–89, 1999.

[19] VDI Gesellschaft. *VDI Wärmeatlas*. Berlin: Springer, 2013.

[20] World Health Organization and UNICEF. Progress on sanitation and drinking-water 2013 update: Joint monitoring programme for water supply and sanitation, 2013.